MAGNETIC RESONANCE TECHNIQUES

Recoupling of Dipolar Interactions in Solid State MAS NMR by Simultaneous Frequency and Amplitude Modulation

Fu, R., NHMFL
Smith, S.A., NHMFL
Bodenhausen, G., Départment de Chimie, Ecole Normale Supérieure, Paris, France

Measurement of dipolar-dipolar interactions between nuclear spins is one of the most universal approaches toward the determination of molecular structure. To obtain high resolution solid state NMR spectra, magic angle spinning (MAS) is required, but MAS removes the weak dipolar interactions between dilute spins. A variety of MAS techniques[1,2] have therefore developed to restore such interactions. These experiments, however, become difficult to accomplish when high spinning speeds are desirable to suppress chemical shift anisotropy, a particularly acute problem in high field spectrometers.

In this report, we proposed a new approach that aims at the reintroduction of the heteronuclear dipolar coupling under fast MAS by radiofrequency (RF) irradiation. The carrier frequency of one of the spins (e.g. S spin) is modulated cosinusoidally while its RF amplitude is modulated as a sine wave. Since the carrier frequency and the RF amplitude are modulated in a periodic fashion, we refer to the new method as "simultaneous frequency and amplitude modulation" (SFAM). It is shown by simulations and experiments that the recoupling by the SFAM is insensitive to RF inhomogeneity (Figure 1) and very effective at high spinning

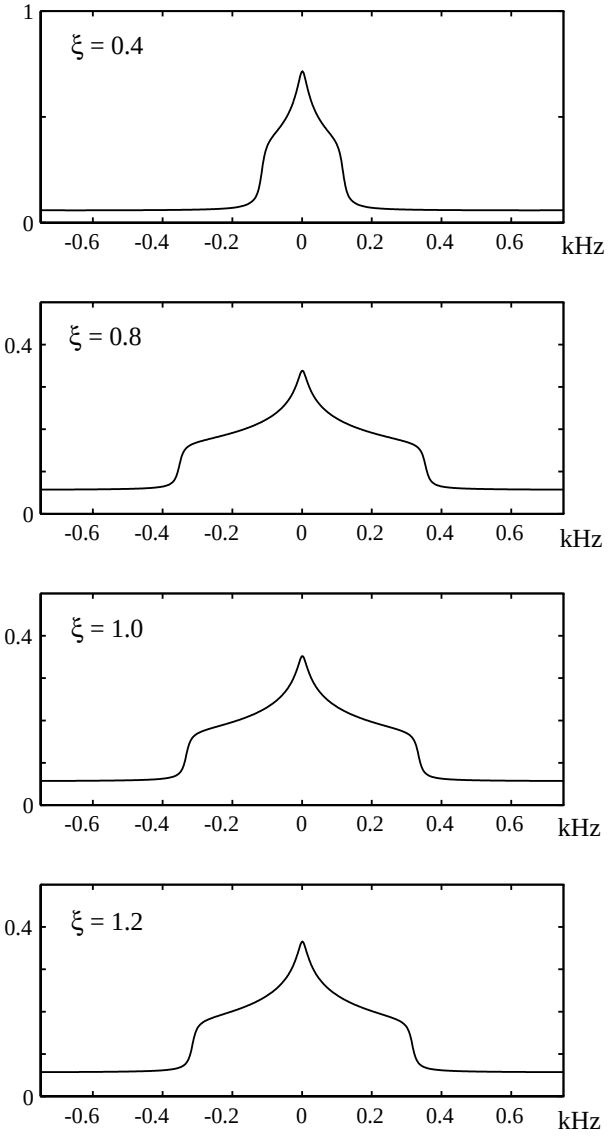

Figure 1. Simulated dipolar powder patterns under the SFAM. The parameters of the *IS* spin system used in the simulations were $D/2\pi$ = 950 Hz and J = 15 Hz. The average carrier frequency was assumed to coincide with the Larmor frequency of the *S* spin. The system was assumed to be spinning at the magic angle at 5 kHz. The parameters used for SFAM were modulation frequency $\omega_{mod}/2\pi$ = 5 kHz (equal to the spinning speed), depth of the frequency modulation $\omega_{\Delta}/2\pi$ = 40 kHz, and RF amplitude $\omega_{1S}^{max}/2\pi$ = 16, 32, 40, and 48 kHz, corresponding to ratios $\xi = \omega_{1S}^{max}/\omega_{\Delta}$ = 0.4, 0.8, 1.0, and 1.2. A 65 Hz line broadening was used in all simulations.

speeds (Figure 2), whereas the well-know REDOR[2] becomes insufficient due to the pulse imperfection effects.

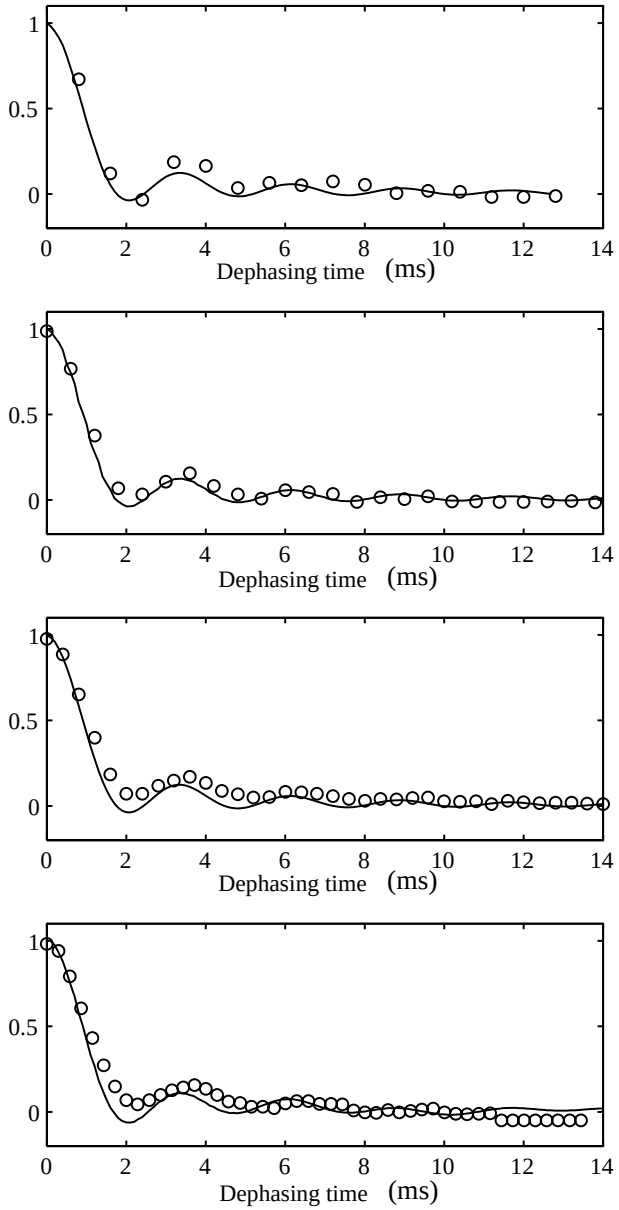

Figure 2. Dephasing of the magnetization of the *I* spins when the *S* spins are irradiated by the SFAM sequence, recorded with different spinning speeds. From top to bottom: $\omega_r/2\pi$ = 2.5, 3.3, 5.0, and 7.0 kHz. The experimental data were shown by open circles. The simulated curves (solid lines) were obtained with parameters $\omega_{mod}/2\pi$ = 40 kHz, $\omega_{1S}^{max}/2\pi$ = 28 kHz (i.e. ξ = 0.7), and the modulation frequency was equal to the spinning speed. Simulations at the given parameters indicate that the dipolar modulation patterns remain essentially independent on spinning frequency up to 18 kHz (not shown here).

References:

1 Oas, T.G., *et al*., J. Chem. Phys., 89, 692 (1988).
2 Gullion, T., *et al*., J. Magn. Reson., 81,196 (1989).

TOESY: A New Technique for Detecting Slow Dynamic Exchange Near Structural Phase Transitions

Fu, R., NHMFL
Klymachyov, A.N., FSU, Chemistry
Bodenhausen, G., Départment de Chimie, Ecole Normale Supérieure, Paris, France
Dalal, N.S., NHMFL/FSU, Chemistry

High resolution solid state nuclear magnetic resonance (NMR) is rapidly becoming an important technique for probing the molecular mechanism of cooperative phenomena such as ferroelectric and antiferroeletric phase transitions. There is, however, an everlasting quest for additional enhancement in the spectral resolution, since the transition mechanisms generally involve only minute changes in ionic sizes and orientations, and lattice and molecular dynamics.

In this report, we describe a novel two-dimensional Cross Polarization combined with Magic Angle Spinning (CPMAS) temperature-jump NOESY technique, abbreviated TOESY, and its applications in detecting slow dynamic processes in the close vicinity of the structural phase transitions. Squaric acid ($H_2C_4O_4$) was chosen as a model compound and the measurements were made in the vicinity of its antiferroelectric phase transition at 100 C. It is demonstrated that TOESY enhances the spectral resolution significantly, which is crucial for distinguishing between several different models of proton dynamic exchange in squaric acid. With the TOESY technique, a multiple structure of the so-called "central peak" in the vicinity of the structural phase transition in squaric acid has been observed for the first time,

as shown in Figure 1. The proton exchange models are established thereafter to analyze the formation of the multiple structure. This study thus shows that the TOESY method has a high potential for opening a new way of detecting slow dynamics and subtle changes in atomic reorientations accompanying structural and other phase transitions.

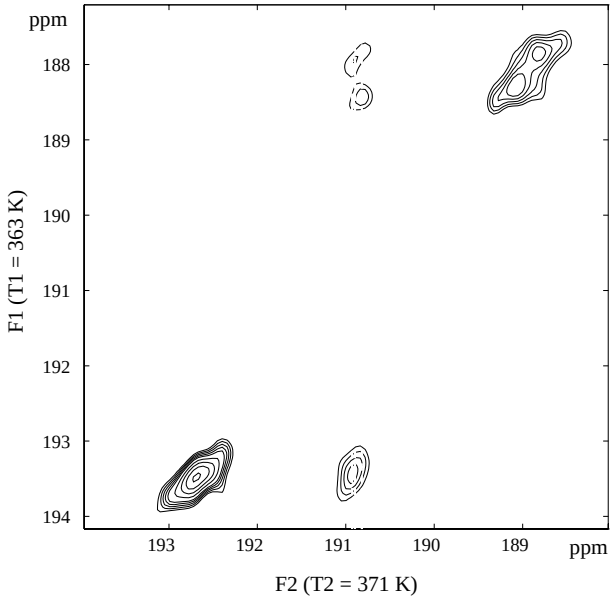

Figure 1. ^{13}C CPMAS 2D TOESY spectrum of a squaric acid crystal where the temperature in the t_1 domain was stabilized at T1=363 K, while the temperature in the t_2 domain was about 371 K. The mixing time for the temperature jumping was about 35 seconds. The sample was spun at 6.0 kHz. In this experiment, 32 scans were used for each t_1 increment. The recycle time was more than ten minutes in order to assure the stabilization of the T1 temperature. The experiment was carried out on a Bruker DMX-300 spectrometer.

References:

1 Klymachyov, A.N., *et al*., Solid State Nucl. Magn. Reson., 7, 127 (1996).

Linear Prediction Cholesky Decomposition vs. Fourier Transform Spectral Analysis for Ion Cyclotron Resonance Mass Spectrometry

Guan, S., NHMFL/FSU, Chemistry
Marshall, A.G., NHMFL/FSU, Chemistry

The fast Fourier transform (FFT) method of spectral analysis converts a time-domain signal to a more easily visualized frequency-domain spectrum, but does not distinguish between signal and noise, and produces spectral artifacts (e.g., "Gibb's oscillations") for a truncated and/or improperly sampled time-domain signal. For example, FFT cannot resolve two signals if the sampling duration is less than one cycle of the frequency difference between the two signals. Here,

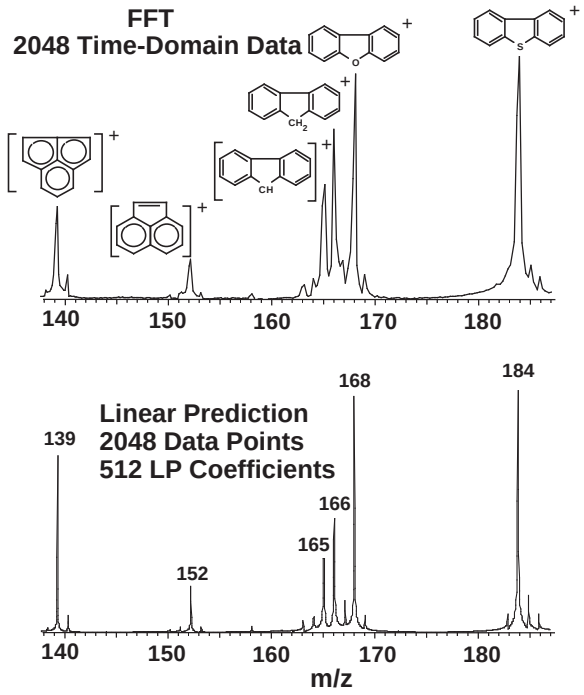

Figure 1. ICR mass spectra obtained by FFT (top) and LP (bottom) methods on the (same) time-domain data. Note that LP resolves the small peak at m/z 183 that is invisible in the FFT spectrum. Also, the peak width in the LP spectrum is significantly lower than that in the FFT spectrum due to time-domain signal truncation.[1]

linear prediction Cholesky decomposition spectral analysis is applied to ion cyclotron resonance mass spectrometry. The algorithm is robust and capable of extracting spectral parameters (frequency, time-domain exponential damping constant, magnitude, and phase) from a signal consisting of multiple exponentially damped noisy sinusoids. Compared to fast Fourier transform data reduction, linear prediction can offer significantly increased sensitivity (for signals at or below the rms noise level), elimination of Gibb's oscillations, and increased spectral resolving power for a time-domain signal that is either truncated or that has damped to the rms noise level before the end of the time-domain acquisition period.[1] The present analysis can handle up to 8K time-domain data sets with 2.5 h PC computation time.

References:

1 Guan, S., *et al*., Anal. Chem. 69, 1156-1162 (1997).

A Combined Linear Ion Trap for Mass Spectrometry

Huang, Y., NHMFL
Li, G.-Z., NHMFL
Guan, S., NHMFL/FSU, Chemistry
Marshall, A.G., NHMFL/FSU, Chemistry

We have proposed a novel ion cyclotron resonance ion trap capable of confining ions even at high pressure.[1] The trap (Figure 1) consists of three capacitively-coupled axial sections, each composed of four circular cross-section rods parallel to the magnetic field axis. Ion confinement along the magnetic field direction is provided by applying the same static voltage to each set of "end-cap" rods. As for a two-dimensional quadrupole mass filter, a sufficiently high rf frequency (several MHz) leads to an "effective" electrostatic "pseudopotential" well with a minimum on the trap central axis. Ions are confined radially by the combination of an applied axial static magnetic field and a radially inward-directed electric field resulting from differential rf voltages applied to each set of four rods. Ion confinement properties are revealed from a Paul trap-like "stability diagram", whereas ion trajectories are analyzed in terms of Penning-type ion cyclotron rotation, magnetron rotation, and axial oscillation motional modes. Ion cyclotron frequency increases with the strength of the rf trapping field. Ion magnetron motion becomes stable if the rf voltage is high enough. Therefore, ion trajectories can be stable even in the presence of ion-neutral collisions. Adding an a.c. potential to a Penning trap should dramatically increase the upper mass detection limit. Following its publication,[1] this work was featured in *Analytical Chemistry*.[2]

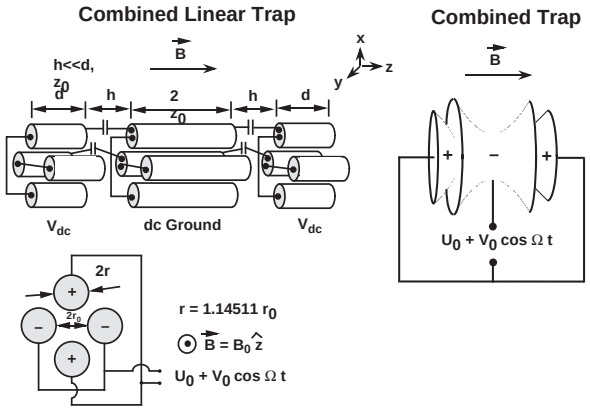

Figure 1. Configurations of a linear "combined" ion trap (left) and "combined" ion trap (right). r is the radius of each quadrupole rod. The optimal ratio, $r/r_0 \approx 1.14511$, has recently been established from exact expressions for the multiple potential expansion. B is the magnetic field inductance; U_0 is dc voltage amplitude; V_0 and w are the amplitude and frequency of the applied rf voltage. V_{dc} is the static voltage applied to the end-section rods to confine ions axially.[1]

References:

1 Huang, Y., *et al.*, Am. Soc. Mass Spectrom. 8, 962-969 (1997).
2 Anal. Chem., 69, 649A (1997).

Linearity and Quadrupolarity of Tetragonal and Cylindrical Penning Traps of Arbitrary Length-to-Width Ratio

Jackson, G.S., FSU, Chemistry
Canterbury, J.D., FSU, Physics
Guan, S., NHMFL/FSU, Chemistry
Marshall, A.G., NHMFL/FSU, Chemistry

The two most popular Penning traps in use for Fourier transform ion cyclotron resonance mass spectrometry (FT-ICR MS) are tetragonal (i.e., orthorhombic with square cross-section) and cylindrical. Here, we compare tetragonal and cylindrical traps as a function of aspect (length-to-width) ratio and position within the trap, by comparing the numerically computed (from Simion 6.0) electric potential field of a given trap relative to each of three idealized potentials required for FT-ICR experiments: dipolar one-dimensional potential for a.c. excitation/detection of cyclotron motion (Figure 1); azimuthal two-dimensional quadrupolar potential for a.c. excitation for ion axialization; and axial three-dimensional quadrupolar potential for d.c. axial confinement of ions. Our numerically computed results agree well with those previously derived analytically. The numerical approach provides a simpler and more accessible means for analyzing the aforementioned potentials. Moreover, the numerical approach (unlike the analytical approach) readily extends to traps of lower symmetry. Finally, even when analytical solutions are available, the numerical method presented here is complementary, since it provides a useful check on the validity of the derived equations.

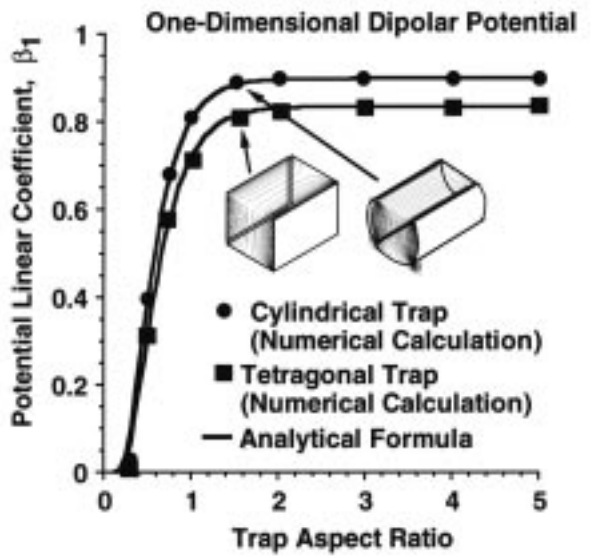

Figure 1. Dipolar potential numerically computed (from Simion isopotential contours) linear coefficient, β_1, for a tetragonal (■) or cylindrical (●) Penning trap (evaluated at the trap midline (y = z = 0) as a function of trap aspect (length-to-width) ratio. For comparison, the smooth curve in each case is computed directly from analytical expressions for β_1. The close agreement between numerical and analytical results validates the analytical formulas.[1]

References:

1 Jackson, G. S., *et al.*, J. Am. Soc. Mass Spectrom. 8, 283-293 (1997).

Sympathetic Cooling of Trapped Negative Ions by Self-Cooled Electrons in an FT-ICR Mass Spectrometer

Li, G.-Z., NHMFL
Guan, S., NHMFL/FSU, Chemistry
Kim, H.S., FSU, Chemistry
Marshall, A.G., NHMFL/FSU, Chemistry

Hot electrons confined in a Penning trap at 3 T self-cool to near room temperature (~0.02 eV) in ~ 1 second by classical radiative emission of cyclotron radiation. This year, we showed that such cold electrons can "sympathetically" cool, in ~10 seconds, laser desorbed/ionized translationally hot Au^- or C_{70}^- ions (see Figure 1) confined simultaneously in the same Penning trap. Unlike "buffer gas" cooling by collisions between ions and neutral gas molecules, sympathetic cooling by electrons is mediated by the mutual long-range Coulomb interaction between electrons and ions,

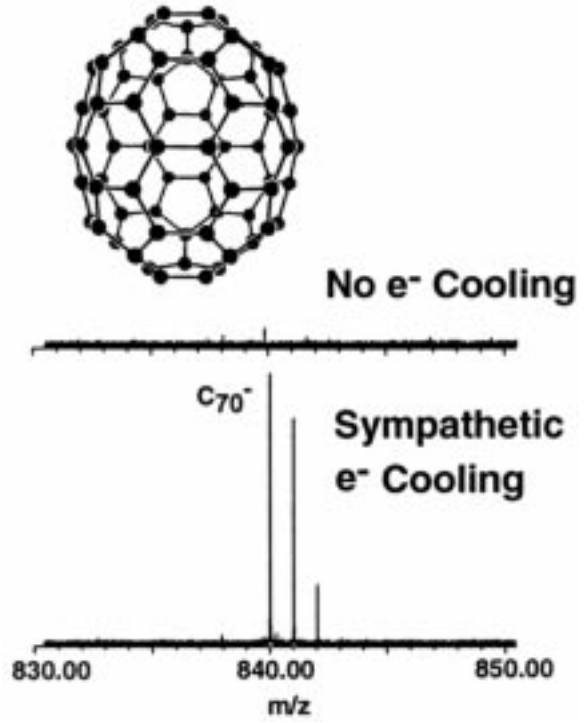

Figure 1. Negative C_{70}^- ions, without (top) and with (bottom) sympathetic cooling by trapped electrons.

so that translationally hot ions can be cooled without internal excitation and fragmentation. We propose that electrosprayed multiply-charged macromolecular ions can be cooled sympathetically, in the absence of ion-neutral collisions, by self-cooled electrons in a Penning trap.

We also applied the cooling method to attach self-cooled electrons to gas-phase neutrals of low electron affinity. Cold electrons have high cross-section for attachment to gaseous neutrals of quite low electron affinity (<0.5 eV). Because both electrons and negative ions may be trapped simultaneously in a Penning trap, the negative ions so formed may be detected by FT-ICR mass spectrometry in the same Penning trap. Compared to conventional chemical ionization, the present method for producing negative ions requires no additional chemical reagent and can be conducted at relatively low pressure by use of pulsed-gas introduction of the sample. We demonstrated the method by successful electron attachment to polycyclic aromatic hydrocarbons with electron affinities as low as 0.49 eV (anthracene) and 0.45 eV (pyrene).[2] That work was subsequently featured by *Analytical Chemistry*.[3]

References:

1 Li, G.-Z., *et al*., J. Am. Soc. Mass Spectrom., 8, 793-800 (1997).
2 Li, G.-Z., *et al*., J. Am. Chem. Soc., 119, 2267-2272 (1997).
3 Anal. Chem., 69, 278A (1997).

A New Probe for Surfaces: Multiple Quantum Filtered ^{131}Xe NMR Spectroscopy

Meersmann, T., NHMFL
Haake, M., Univ. of California at Berkeley, Chemical Engineering
Deschamps, M., Ecole Normale Supérieure, Paris, France
Bodenhausen, G., Ecole Normale Supérieure, Paris, France
Cros, F., Ecole Polytechnique, Palaiseau, France

The interface between solid surfaces and cavities filled with gaseous ^{131}Xe can be probed by multiple-quantum filtered (MQF) NMR. Physisorbed ^{131}Xe is usually not directly observable by NMR spectroscopy, but information can be transferred into the gas phase through desorption.

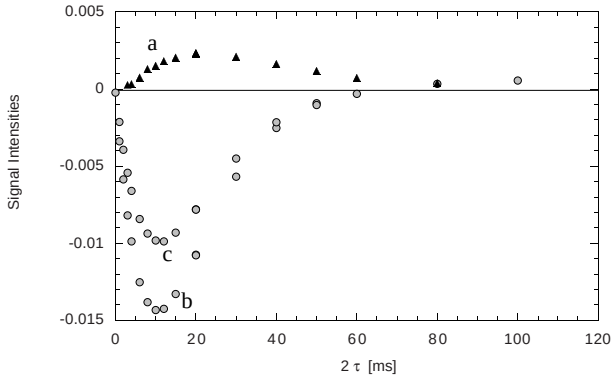

Figure 1. Various MQF curves for xenon-131 inside an Aerogel host structure. (a) Triple quantum filtered, (b) double quantum filtered and (c) a modified double quantum filtered xenon-131 NMR spin echo envelope. The occurrence of the curve (c) is an indication for local confinement of the xenon-surface interaction in this system.

The exchange process may lead to higher-rank order of the nuclear spins in gaseous xenon which can be detected by MQF-NMR.

This new technique has been applied for the first time to study the surfaces of aerogels that are of particular interest in material sciences. The MQF spectra show a strong dependence on the type of aerogel used for the experiment. They also provide a sensitive measure for water adsorbed on the aerogel surfaces.

NMR Spectroscopy in Anisotropic Gas Phase: Xenon-131 Quadrupolar Splitting at High Magnetic Fields

Meersmann, T., NHMFL
Haake, M., Univ. of California at Berkeley, Chemical Engineering

At very high magnetic fields strengths (≥ 14 T) the xenon-131 gas phase NMR spectrum shows a well resolved quadrupolar splitting. Quadrupolar coupling of a non-spherical (S > 1/2) nuclei with an electric field gradient will occur when the electrical isotropy of the surrounding electron cloud is disturbed. The experimental results suggest that the origin of the observed splitting in the gas phase is twofold. A largely field independent portion arises from the interaction of the xenon with the gas container wall (i.e. Pyrex tube). In addition, a field dependent splitting is present, leading to a splitting of 3.9 Hz at 720 MHz field strength. Comparison with multiple quantum filtered NMR of liquid xenon demonstrates that the field dependent portion does not originate from surface interactions.

The discovery of a surface independent quadrupolar splitting indicates that an electrical polarization of the xenon electron cloud is induced by the magnetic field.

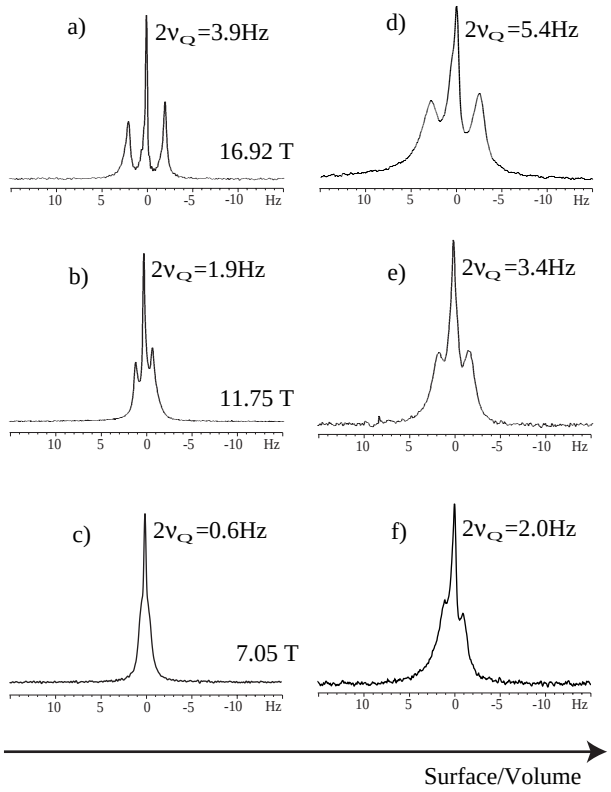

Figure 1. Gas phase xenon-131 NMR spectra at three field strengths and two different surface conditions. a), b), c): The Xenon is contained in a plain Pyrex glass tube with 6 mm i.d. d), e), f): Increased surface areas due to capillaries added into the Pyrex tube. All experiments were recorded at 305 K and 0.4 MPa (4 atm) xenon pressure.

Xenon-131 Imaging of Aerogels in High Temperature Liquid Phase

Meersmann, T., NHMFL
Pavlovskaya, G., NHMFL
Blue, A., NHMFL
Gibbs, S., NHMFL/FAMU-FSU College of Engineering
Haake, M., Univ. of California at Berkeley, Chemical Engineering
Cros, F., Ecole Polytechnique, Palaiseau, France

In recent years, gas-phase imaging utilizing optically pumped xenon-129 has received a great deal of attention for medical applications, for example in lung imaging. This report is about the other NMR active isotope (i.e. xenon-131) that exhibits distinctive features for imaging

applications in material sciences that are not obtainable from xenon-129. The relaxation times of xenon-131 in gas and liquid phases depend strongly on the surface of the surrounding materials thus leading to a substantial dispersion of relaxation rates. In aerogels—i.e. materials with low density (around 0.1 g/cm^3) and large surface areas—the relaxation time T_1 decreases from around 110 ms outside the aerogel cavities to 27 ms inside the cavities. Removal of the surface bound water from the aerogel leads to even faster relaxation (T_1 = 7 ms), which may be used to yield a surface specific contrast for imaging. The experiments were performed at very high fields (600 MHz for protons or 49 MHz for xenon-131) in order to overcome the sensitivity problems of xenon-131 since optical pumping is not an option due its fast relaxation. In addition liquid xenon close to the critical point (289 K) was chosen, thus providing a high spin density in addition to gas-like relaxational behavior. The potential of this isotope as a contrast agent is demonstrated in Figure 1.

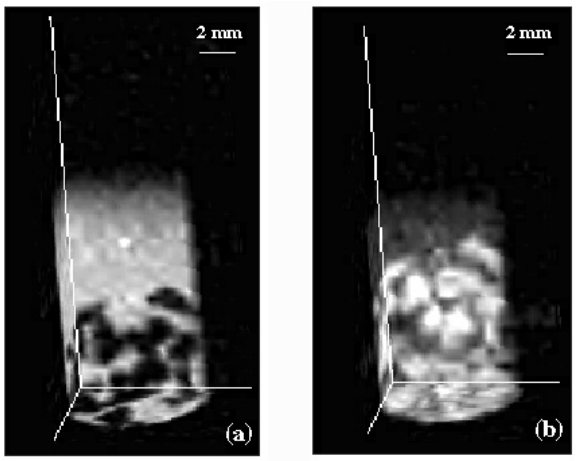

Figure 1. Images of liquid xenon-131 (natural abundance) outside (a) and inside (b) an aerogel. (a): A long relaxation delay (D1 = 400 ms) and long echo time (20 ms) leads to the suppression of the xenon-131 spins that are in close contact with the aerogel. (b): Opposite effect for short relaxation delays and short echo times.

Dispersion in Chromatography Studied by Pulsed Field-Gradient NMR

Park, J. K., NHMFL/FAMU-FSU College of Engineering
Coffman, J.L., BioSepra Inc.
Gibbs, S.J., NHMFL/FAMU-FSU College of Engineering

Axial mixing or dispersion in the flow direction reduces resolution in packed column chromatography. The overall dispersion is often characterized by the plate height H, which can be measured in an impulse-response experiment from the width of the Gaussian response curve. Several factors including adsorption kinetics, surface diffusion, pore diffusion, interphase mass-transfer resistance, and convective dispersion all contribute to the total plate height, and hence it is difficult to unambiguously determine individual effects in a small set of experiments. Measuring the impulse response for a range of evolution times, for which the response may not be Gaussian, may allow separation of the contribution of these individual effects. A better understanding of these effects may lead to improved separation design and performance.

Pulsed field-gradient (PFG) NMR allows the measurement of displacement spectra over time intervals ranging from a few milliseconds to a few seconds. For flow in porous media, such as chromatographic columns, these displacement spectra may be analyzed to help understand details of the convective dispersion process, in particular, its time dependence and approach to Gaussian behavior. In combination with magnetic resonance imaging methods, PFG techniques may allow the measurement of the spatial dependence of fluid velocity and dispersion in packed columns and other porous media.

Displacement spectra obtained in 1997 using the 600 MHz 89 mm bore microimaging NMR

spectrometer in Tallahassee for water flow in packed beds of 780 um diameter and 99 um diameter polystyrene beads and of 50 um diameter porous polyacrylamide beads demonstrate the concepts described above and show a large time-dependence of the effective axial dispersion coefficient for short times corresponding to fluid displacements of less than ten particle diameters. Examples of displacement spectra for different effective dispersion times and for 99 um diameter polystyrene beads are shown in Figure 1.

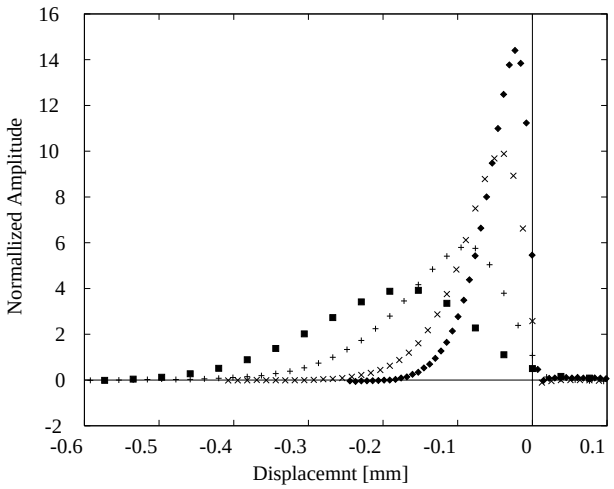

Figure 1. PFG NMR displacement spectra corresponding to dispersion times ranging from 10 ms to 100 ms for water flowing in a column packed with 99 um diameter polystyrene beads. Note the asymmetric spectra.

Further work should address reproducibility of observations in order to quantitatively correlate the time-scales for approach to Gaussian behavior with system parameters. Spatially resolved measurements of velocity and dispersion are in progress, but the results obtained to date suggest caution in the use of so-called phase mapping techniques for velocity imaging since displacement spectra may be highly asymmetric especially for short displacement times.

Applications of Magnetic Resonance Imaging Velocimetry to Flow in Porous Media and Fiber/Composite Manufacturing

Pavlovskaya, G., NHMFL
Han, K., FAMU-FSU College of Engineering
Park, J.K., NHMFL/FAMU-FSU College of Engineering
Gibbs, S.J., NHMFL/FAMU-FSU College of Engineering

Work in 1997 has focused on implementation of MRI velocimetry on the 600 MHz 89 mm bore microimaging NMR spectrometer in Tallahassee and on fabrication of model porous media for investigation of the effects of a transverse permeability discontinuity on flow fields.

Flow in heterogeneous porous media occurs in a great variety of situations including biology, geophysics, and engineering. Improved understanding and more efficient modeling of such flows may lead to improved processes of polymer-fiber composite manufacturing, for example.

Techniques have been developed for binding monodisperse polystyrene beads with a thin coating of polyester resin in a precision annular form in order to obtain a simple model system for investigation of the effect of the porous medium permeability on the central channel flow. Work to characterize the structure of the resulting porous media by high resolution three dimensional MRI is in progress.

Protocols and data analysis software for pulsed field-gradient MRI velocimetry of Poiseuille flow in a cylindrical tube have been implemented and tested for water flow in a 5 mm precision internal diameter glass tube. These data are presented below and suggest implementation of the methods for more complex geometries.

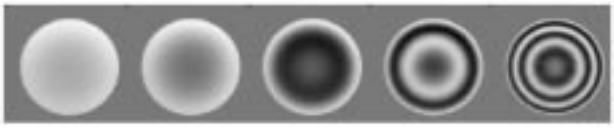

Figure 1. Phase-encoded flow 256 x 256 pixel MRI images for Newtonian flow in a 5 mm ID glass tube. Images obtained at 600 MHz.

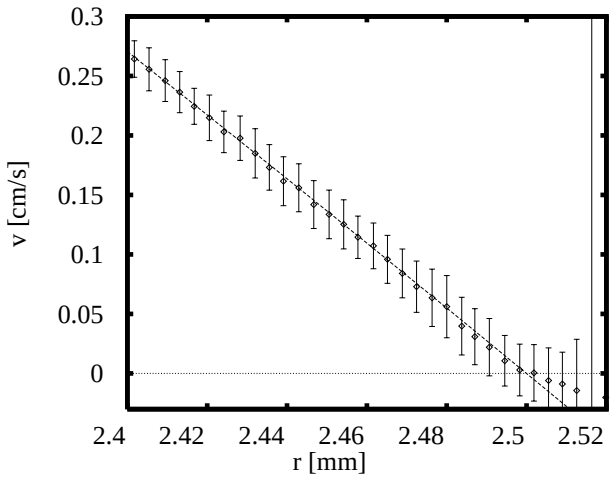

Figure 2. Azimuthally averaged velocity profile for the wall region obtained from analysis of the images in Figure 1. The line is the expected parabola and the points are averages of 50 MRI points in a radial bin. The effective spatial resolution is finer than 4 um.

Magnetic Resonance Imaging of Foams

Prause, B.A., Univ. of Notre Dame, Physics
Gibbs, S.J., NHMFL/FAMU-FSU College of Engineering
Glazier, J.A., Univ. of Notre Dame, Physics

We continue to explore applications of high field NMR microimaging to study the structure and coarsening dynamics of liquid foams. An example of results obtained using the 600 MHz microimaging spectrometer in Tallahassee for liquid gelatin foams is shown in Figure 1. During 1997, $CuSO_4$ and $DyCl_3$ doping of the liquid foams was optimized to obtain the narrowest possible NMR linewidth for the foams at 600 MHz. In addition, temperature control of the liquid foam was implemented while imaging in order to control the foam coarsening rate.

Analysis of the images to obtain bubble sizes and connectivities as a function of coarsening times is in progress. The availability of larger acquisition bandwidths (faster digitizers) would enable improved image quality for these large bandwidth systems.

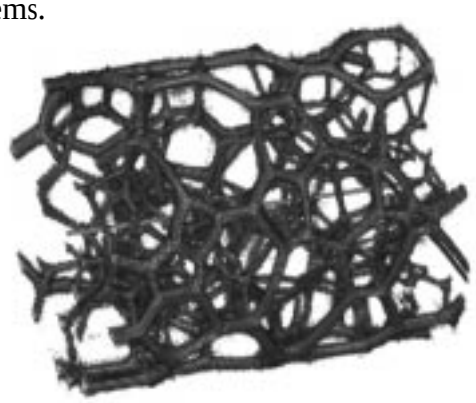

Figure 1. Isosurface rendering of 3D magnetic resonance image of a Dy and Cu doped liquid gelatin foam in which cell faces are suppressed in post-acquisition processing. Resolution: 86 um. Acquisition time 2:44 hours. Image obtained with a spin-echo "spin-warp" imaging sequence at 600 MHz. Field of View: 11 mm.

Helix Parameters and Chemical Shift Tensors

Quine, J.R., FSU, Mathematics/NHMFL
Denny, J., FSU, Mathematics/NHMFL
McNiel, S., FSU, Mathematics/NHMFL

The study of proteins and polypeptides using solid-state NMR requires the use of mathematical analysis to find protein structures compatible with the data. In an earlier study[1] it was shown that the orientations of bond directions in the peptide plane determine the backbone structure except for a sequence of chiralities (+1 or -1), one for each peptide plane and α-carbon.

It is also important to analyze the situation where not enough information is available to give the orientation of each bond. One example is when a single chemical shift is known in several peptide planes. In this study we are concerned with using the data from ^{15}N chemical shift experiments on the backbone of a transmembrane protein to

determine the tilt of the helices in an α-helix bundle. In particular, we are interested in the transmembrane segment of the M2 transmembrane protein studied by Kovacs and Cross.[2] In the initial stages of structure determination, certain assumptions are made concerning the parameters of the helix such as radius, residues per turn, and whether the helix is regular, bent or kinked. In all cases it is important to know the direction of the helix axis in the molecular coordinates of the peptide plane. Formulas relating all the parameters in question have been found using a model of a helix as the orbit of an initial peptide plane under a repeated applications of a single screw rotation.[3] The axes of the chemical shift tensor are known in the peptide plane, and the values of the tensor in the principal axis directions are found from powder pattern experiments. From a sequence of chemical shifts along the backbone, a system of equations is obtained whose solution gives the angle between the helix axis and the magnetic field direction as well as the projection of the magnetic field direction onto a helical wheel for the α-helix.

For the M2 transmembrane protein, a substantial tilt of about 35° is found. Presumably this is because of the angle between helix axes required when two α-helices pack together in a 4-4 packing. Mathematical models of four helix bundles are being formulated to determine the proper set of parameters to give the required length to span the membrane and the proper diameter for the channel.

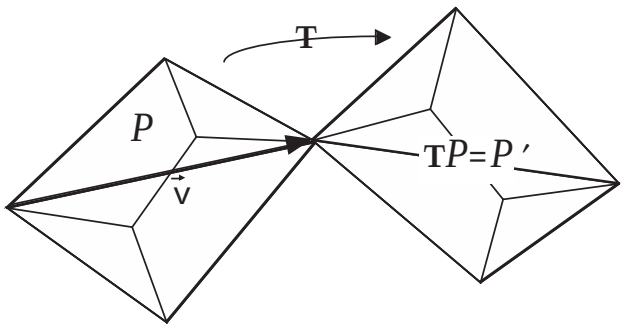

Figure 1. The transformation that sends one peptide plane to the next is a screw rotation of the form Tx=Ax+v, where *A* is a rotation and *v* is the virtual bond vector.

References:

1 Quine, J.R., *et al.*, Biophysical Journal, 72, 2342-2348 (1997).
2 Kovacs, F.A., *et al.*, Biophysical Journal, 73, 2511-2517 (1997).
3 Quine, J.R., preprint.

NMR Imaging of ^{14}N in Solids by the Stray Field Technique

Randall, E.W., Queen Mary & Westfield College, Chemistry, London, England
Samoilenko, A.A., Institute of Chemical Physics, Russian Academy of Sciences
Fu, R., NHMFL

The ^{14}N isotope has been imaged in *solutions* of nitrogen compounds by conventional methods both directly,[1] and indirectly by a $^{1}H\{^{14}N\}$ decoupling method[2] and by spin echo double resonance.[3] These techniques, which involve switched gradients, are successful, however, only for relatively narrow lines of the order of 1 kHz or less, mainly because induced eddy currents in unshielded sets limit the quick recording of data after the pulse. The technique that has had quite spectacular success for the NMR imaging of broad lines even for example in crystalline solids, both diamagnetic and paramagnetic, is the stray field (STRAFI) imaging method. This utilizes the very large *static* gradients in the stray fields of high field magnets. It has proved to be successful even for quadrupolar nucleides. These have been confined so far, however, to those with half-integral spin.[4,5] The spectrum of each of these nuclei contains a relatively narrow transition (1/2 to -1/2), characterized by a linewidth, which to first order, is given by Cq^2/n, where Cq is the electric quadrupole coupling constant, and *n* is the Larmor frequency. This is typically of the order of kHz, and is little more than the width associated with dipole-dipole interactions, so that it poses no problems for STRAFI imaging. Such narrow central transitions are absent, however, in the spectra of nucleides having integral spins such as ^{2}H, ^{14}N (each with I = 1) and ^{10}B (I = 3), and it is

to these nuclei that we turned for a more exacting test of STRAFI methods.

We have already successfully tested the feasibility of generating Hahn echoes in the STRAFI spectroscopy of ^{2}H, and therefore of generating STRAFI images. The electric quadrupole moment of ^{2}H, however, is relatively small and so are the values for Cq. We decided on a severer test of the STRAFI method by using compounds of ^{14}N in which values of Cq can range from near zero to 5 MHz or more, so that the powder patterns are very wide indeed.

In this report, we have observed Hahn echoes resulting from Powles-Mansfield pulse sequences from a variety of nitrogen containing solids, which exhibit a range of ^{14}N electric quadrupole coupling constants (C_q) up to 4.9 MHz on a Bruker DMX WB 600 equipped with a Magnex magnet of bore 89 mm. One dimensional profiles are presented for solid ammonium nitrate and sodium nitrite, and the spatial resolution is discussed as a function of C_q.

References:

1 Kinchesh, P., *et al*., Magn. Reson. In Chem., 31, 495 (1993).
2 Kinchesh, P., *et al*., J. Magn. Reson., 100, 625 (1992).
3 Kinchesh, P., *et al*., J. Magn. Reson. Series B, 105, 253 (1994).
4 Bodart, P., *et al*., accepted for publication, Solid State NMR.
5 Samoilenko, A.A., Proceedings of the Ampere Conference, Canterbury (1996).

Optical Pumping and Nuclear Spin Diffusion in Bulk GaAs and GaAs/AlGaAs Superlattices

Reno, J.L., Sandia National Laboratories
Simmons, J.A., Sandia National Laboratories
Vitkalov, S., UF, Chemistry
Bowers, C.R., UF, Chemistry

Last year we reported a study of the field dependence of the optical Overhauser effect in bulk GaAs that was performed at the NHMFL resistive magnet facility.[1] The field dependence of the total ^{69}Ga nuclear magnetization was modeled using a diffusion-scalar relaxation equation. From modeling of the field, time and polarization dependence of this macroscopic observable, a microscopic interpretation of the optical Overhauser effect near shallow donor sites in GaAs also emerges.[2] Using the numerical solutions that best fit the available data, the spatial dependence of the nuclear Zeeman order and the hyperfine frequency shift can be derived and used in simulations of the time evolution of the ^{69}Ga NMR line shapes. These simulations provide guidance about how to optimize the experimental conditions to most effectively observe hyperfine effects near shallow donors in this particular material.

We have now extended our optically pumped NMR studies to multiple GaAs/AlGaAs quantum wells. Interest in such experiments is due to recent NMR Knight shift and spin lattice relaxation measurements that have provided new insight into the possible formation of charged spin texture excitations (i.e. Skyrmions) in the context of the quantum Hall effect. Although the observable nuclei in these NMR experiments (^{69}Ga, ^{71}Ga and ^{75}As) all possess a quadrupole moment, no quadrupole splitting is observed due to the cubic symmetry of the lattice. We demonstrate that uniform and controlled strain can be useful to identify optically pumped NMR signal contributions from different layers in the sample and to determine the nuclear spin polarization. The orientation of the quadrupole coupling tensor with respect to the crystal axes was determined by a rotation study. A uniform biaxial strain in the plane of wells can be induced by epoxy bonding of the GaAs/AlGaAs multilayer structure to a Si (100) support. The result is a quadrupole splitting of 55 kHz at 1.5 to 4.2 K. Differences in the spin lattice relaxation of the central versus satellite transitions of the ^{71}Ga signal are attributed to quenching of spin diffusion at the GaAs/AlGaAs boundary. Spin diffusion into the barrier regions influences the apparent nuclear spin lattice relaxation time in the wells, an effect we have modeled with the relaxation-diffusion equation. These calculations may be beneficial in NMR studies of the QHE.

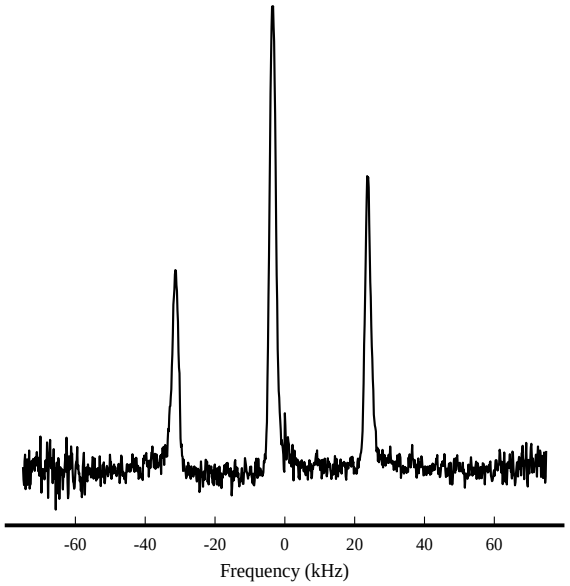

Figure 1. The 91.5 MHz gallium-71 NMR spectrum of a strained GaAs/AlGaAs multiple quantum well sample oriented at 35 degrees with respect to the magnetic field. Optical pumping signal enhancement was employed to record this signal in a single scan at a temperature of 4.2 K.

References:

1 Kuhns, P.L., *et al*., Phys. Rev. B., 55, 7824 (1997).
2 Bowers, C.R., Solid State NMR, in press.

Fabry-Perot Cavity for Multifrequency High Field Electron Paramagnetic Resonance at Microwave Frequencies from 110 GHz to 330 GHz (3.9 to 12 T Magnetic Field)

Rohrer, M., NHMFL
Krzystek, J., NHMFL
Williams. V., NHMFL
Brunel. L.-C., NHMFL

In the course of striving for higher sensitivity of the multifrequency/high field EPR spectrometer at NHMFL, a Fabry-Perot (FP) type microwave (μW) cavity has been developed at the NHMFL. Its design is based on a semiconfocal arrangement of the two cavity mirrors, where the upper one consists of a flat copper mesh that allows for the necessary μW coupling into the FP resonator. The enhancement of the μW fields in the cavity leads to an increased sensitivity. It allows to measure diluted paramagnetic systems and/or smaller sample volumes as compared to the simpler transmission mode of operation, where the μW passes the sample in a single path only. The new FP design has been shown to be operational in the entire temperature range from room temperature to liquid helium temperatures. Samples can be powders, frozen solutions or even liquid solutions.

Test measurements on standard samples clearly show the sensitivity of the spectrometer to be enhanced by about two orders of magnitude; the sensitivity of the NHMFL spectrometer is now of 10^{10} spins per gauss at room temperature and of 10^{8} spins per gauss at liquid helium temperature. Some projects on different paramagnetic systems have been initiated :

(a) Measurements on very small sample volumes (2 μl) of diluted (0.5 mM) nitroxide spin labels. The EPR linewidth and lineshape of these samples in the liquid solution can now be studied in its temperature- and field-dependence, which allows for the elucidation of dynamical processes related to the radical.

(b) Tyrosine (TYR 177) anion radicals from mouse ribonucleotide reductase. The drastically increased Zeeman interaction at the very high fields leads to fully resolved g-anisotropy in the frozen solution spectra, and even partially resolved hyperfine splittings of these biological samples.

(c) Diluted K_3CrO_8 (5 %) in Niobate (K_3NbO_8). This Cr(V) salt is regarded, besides other alkali-metal peroxychromates, as a fundamental example for studying transition metals in their simplest electronic structure. In order to extend these studies on diluted paramagnetic systems containing Cr(V), where no electron spin exchange can take place, the higher sensitivity of the FP-resonator can reveal further insight into the electronic structure.

Thereby, the new FP type μW cavity has been proven to be a powerful tool for a large variety of EPR applications, and several publications are in preparation.

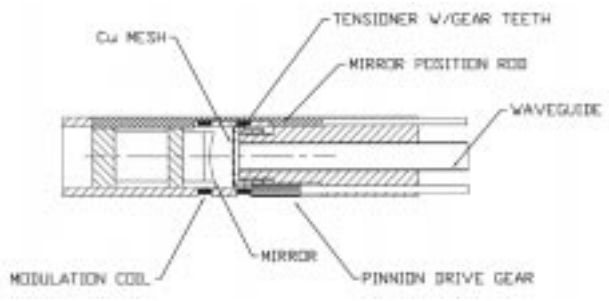

Figure 1. A cross-section of the FP cavity employed in the NHMFL high field EPR spectrometer.

The Effect of Temporal Stability on Biological NMR at High Fields in Resistive Magnets

Sabo, M., NHMFL
Soghomonian, V., NHMFL
Verraneault, R., NHMFL
Cross, T.A., NHMFL/FSU, Chemistry

Temporal stability of the magnetic field is of absolute importance for conducting nuclear magnetic resonance (NMR) experiments. In most biological samples, the duration of a single experiment is on the order of hours. The length of data acquisition is governed by factors such as sensitivity or number of spins of the nucleus of interest. High fields offer a number of advantages including enhanced sensitivity, but these might be offset by the temporal instability associated with these magnets. Experiments that require extensive signal averaging cannot be conducted with fluctuating or drifting magnetic fields. Therefore, the control of the temporal instability is necessary in order to obtain crucial and novel information while probing biological systems.

In resistive magnets, the sources of temporal instability are (a) the inlet temperature of the magnet cooling water, and (b) the power supply stability. A change of 1 ˚C in the temperature of the inlet water causes a 17 ppm shift in the magnetic field. Under normal operating conditions, 2-3 ˚C changes are common. Hence maintaining temperature control during both steady state and transient operation is paramount to performing high resolution NMR experiments with these resistive magnets. If the temperature variation is constrained to 0.3 ˚C, then, with flux stabilization and field frequency lock unit, field fluctuations are held to 1 ppm. The control scheme that was in operation relied on "temperature control" to maintain a given inlet temperature value. Therefore, the temperatures and the differences in temperature of chiller units, heat exchangers, storage tank, and return magnet cooling water all had to be monitored. Based on these data, the uptake of chilled water would vary to maintain the setpoint temperature at the magnet.

Alternatively, different control schemes may be used. "Flow base control" was implemented and comparison tests between the two control schemes were performed. Testing was conducted using two 30 T resistive magnets. One magnet was ramped to 30,000 amps at a ramp rate of 400 amps/second, at 12 MW power consumption. Twenty minutes after this ramp, the second magnet was ramped to 30 T under identical conditions. A temperature setpoint of 9 ˚C for the magnet cooling water was selected for both test sets. The primary concern was to evaluate the efficacy of the control schemes in minimizing the effect of a transient, such as a second magnet ramping, on the inlet temperature of the magnet cooling water of the first magnet.

The results obtained thus far are presented in Figure 1, which depicts the outlet temperature of the heat exchanger, and hence the inlet temperature of the magnet cooling water, during the transient. Data with the original "temperature control" scheme shows a peak temperature excursion of 1.8 ˚C above the setpoint as a result of the second magnet ramping up. The period during which the inlet temperature of the magnet cooling water is outside the 0.3 ˚C of the setpoint is over 700 seconds. Data with "flow base control" scheme results in only 0.7

˚C peak temperature excursion for identical power consumption by the second magnet. Not only is the magnitude of the excursion reduced by a factor of 2.6, but the time duration when the inlet temperature of the magnet cooling water is outside the 0.3 ˚C range is now reduced to 160 seconds. The results demonstrate a greater degree of control now possible over the temperature of the magnet cooling water, and ultimately, control over the temporal instability of the magnetic field. Consequently, these high fields may be utilized to perform NMR experiments on biological systems.

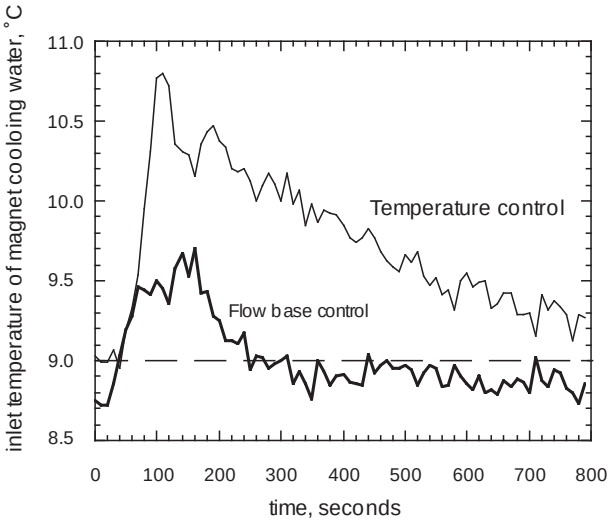

Figure 1. Comparison of "flow base control" vs. "temperature control" schemes employed in maintaining the setpoint temperature of the magnet cooling water.

References:

1 Soghomonian, V., *et al*., J. Mag. Res., 125, 212 (1997).

2 Cross, T.A., *et al*., invited presentation, 38th Experimental Nuclear Magnetic Resonance Conf., Orlando, Florida, March 23-27, 1997.

Stray Field Imaging at High Magnetic Fields

Samoilenko, A.A., Institute of Chemical Physics, Russian Academy of Science
Randall, E.W., Queen Mary and Westfield College, London, Chemistry
Soghomonian, V., NHMFL

The stray-field (STRAFI) imaging method is a useful technique for imaging nuclei with short spin-spin relaxation times. The STRAFI technique utilizes the very large static magnetic gradient at the edge area of a superconducting solenoid. The value of this gradient is related to the central magnetic field value and bore diameter: the narrower the bore and the higher the central field, the larger the gradient. These gradients range from 10 to 50 T m^{-1} for different superconducting magnets. The 19.6 T narrow bore (31.6 mm) magnet at the NHMFL has the highest gradient, measured at 76 T m^{-1}. These large gradients may be employed to image broad spectral lines in solids, liquids, liquids in solids, etc.

Stray field imaging is a slice selective method. A sample is placed in the planar region of the gradient, where the radial field is uniform and the gradient is along the axial direction. This is the sensitive plane. The sample is the excited by radiofrequency pulses of selective frequency. Due to the magnetic field gradient and duration of pulse, information is only obtained from a thin slice of the sample. Thus, moving the sample along the axial, Z, direction provides, in a slice-wise manner, information that can be recombined to give a one-dimensional profile of the sample. Because of the large gradient, the spin-spin relaxation time, T_2^*, of the nuclei becomes so short that the signal decays to zero before it can be recorded. To mitigate the adverse effect of the gradient on the relaxation properties of the nuclei, an echo train is utilized. The introduction of a second pulse after a time interval tau, τ, generates an echo at time 2τ. The intensity of the echo provides the information,

and hence Fourier transformation of the data is not required.

On the 19.6 T system, we applied STRAFI imaging to a variety of half integral nuclei in solids; ^{23}Na in NaCl at 126.2 MHz, ^{31}P in NH_4PF_6 at 193.1 MHz, ^{2}H in D_2O at 73.2 MHz and ^{27}Al in Al_2O_3 at 124.3 MHz. The Al_2O_3 sample was a hollow tube with outer diameter of 6.4 mm and an inner diameter of 3 mm. A tube section of length of 15 mm was placed in the magnetic field with the axial axis of the tube perpendicular to the vertical, Z, axis of the magnet and hence perpendicular to the gradient also. The experimental parameters were two 90˚ pulses with pulse width of 4 μs, tau value of 103 μs, and 100 scans for each vertical position at a 0.2 second recycle delay. The resonance frequency as mention was 124.3 MHz. The vertical translation of the probe was achieved by means of a finely threaded rod. The experimental curve, as well as the calculated one are depicted in Figure 1. The figure represents the variation of the intensity of the signal as the tube is moved through the sensitive plane. As in any other nuclear magnetic resonance experiment, the intensity of the signal is proportional to the number of nuclei sampled. As the sample has a hollow portion, the "amount" of Al_2O_3 material at each vertical position is proportional to the geometry of that particular slice. We expect to see two symmetric horns of maximum intensity when the axial axis of the tube is exactly perpendicular to the gradient. We can also calculate the area of each slice, and that is given by the solid line in Figure 1. The first experimental point was obtained below the sample and we then moved the sample up into the sensitive slice with increments of 0.25 mm. We observed good correlation between experiment and calculated values. Since the spatial resolution of the horns is sharp, we deduce that the line width of the ^{27}Al resonance is quite narrow. This could indicate a highly symmetric Al atom site. Unfortunately, the exact solid state structure of the Al_2O_3 tube is unknown (Omegatite 350).

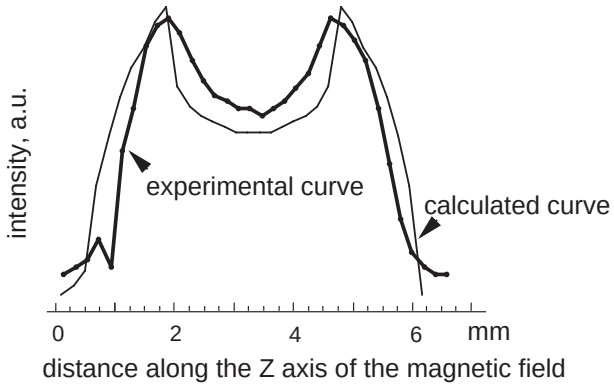

Figure 1. Variation of the intensity of the NMR signal as the tube is moved, along the vertical axis of the magnet, Z, into the sensitive slice. The experimental (heavy) and calculated (light) lines show good agreement, an indication of good spatial resolution obtainable by the STRAFI technique.

These were preliminary experiments conducted on the 19.6 T magnet to probe the feasibility of performing STRAFI at very high fields. The information content as well as the resolution increases with gradient strength, and therefore this system should prove to be very useful for stray field-imaging as well as stray-field spectroscopy.

References:

1 McDonald, P.J., in *Spectroscopy Europe*, 7/8, 25 (1995).
2 Samoilenko, A.A., *et al*., JEPT Lett., 47, 348 (1998).
3 Bodart, P., *et al*., Solid State NMR, 8, 257 (1997).

External Accumulation of Ions for Enhanced Electrospray Ionization Fourier Transform Ion Cyclotron Resonance Mass Spectrometry

Senko, M.W., NHMFL
Hendrickson, C.L., NHMFL
Emmett, M.R., NHMFL
Shi, D.-H.S., FSU, Chemistry
Marshall, A.G., NHMFL/FSU, Chemistry

Electrospray ionization (ESI) in combination with Fourier transform ion cyclotron resonance (FT-ICR) mass spectrometry provides for mass analysis of biological molecules with unrivaled mass accuracy, resolving power and sensitivity. However, ESI FT-ICR MS performance with on-line separation techniques such as liquid chromatography and capillary electrophoresis has to date been limited primarily by pulsed gas assisted accumulation and the incompatibility of the associated pump-down time with the frequent ion beam sampling requirement of on-line chromatographic separation. In work published in 1997,[1] we described numerous analytical advantages which accrue by trapping ions at high pressure in the first octupole of a dual octupole ion injection system (see Figure 1) before ion transfer to an ICR ion trap in the center of the magnet for high performance mass analysis at low pressure. The new configuration improves the duty cycle for analysis of continuously generated ions, and is thus ideally suited for on-line chromatographic applications. We demonstrated LC/ESI FT-ICR MS on a mixture of 500 femtomoles of each of three peptides. Additional improvements include a 5-fold increase in signal-to-noise ratio and resolving power compared to prior methods on our 9.4 T instrument.

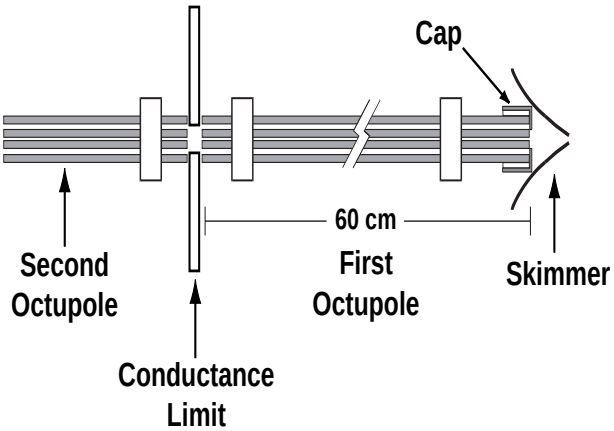

Figure 1. Schematic diagram of an octupole ion guide, in which the front end cap and conductance limit serve as trapping electrodes.

References:

1 Senko, M. W., *et al.*, J. Am. Soc. Mass Spectrom., 8, 970-976 (1997).

Sensitivity Enhancement in NMR as a Function of Magnetic Field Strength

Soghomonian, V., NHMFL
Cross, T.A., NHMFL/FSU, Chemistry

In NMR the search for sensitivity is an ever present challenge. There are ways of increasing the sensitivity by increasing the number of nuclei of interest in the sample, applying magnetization transfer techniques, or increasing the field strength, to mention a few. A measure of the sensitivity in an NMR experiment is given by the signal to noise ratio, S/N. Both the number of acquisitions and instrumentational factors affect the S/N ratio. To measure the effect of magnetic field strength, B_o, on the S/N ratio, a set of experiments was performed at four magnetic field strengths, ranging from 9.4 T to 23.2 T. This represents the highest field strengths for such sensitivity comparisons.

Deuterium spectroscopy greatly benefits from an increase in field strength. Not only is higher S/N ratio observed, but also a decrease in the acoustic ringing problem associated with the relatively low Larmor frequency of this nucleus. The minimization of the acoustic ringing makes the observation of fast relaxing sites possible. However,

for this sensitivity comparison, d_4-alanine was chosen as the model compound, which possesses a long relaxation time. The Pake pattern representing the quadrupolar interaction is field independent. A 10 mg sample was prepared and used to record spectra at 9.4, 14.1, 19.6 and 23.2 T. The same spectrometer, probe, sample, and acquisition parameters, pulse width and recycle delay, were used to record the spectra depicted in Figure 1. The only acquisition parameter that varied in these experiments was the tau value, the interpulse delay, which is influenced by acoustic ringing. At 9.4 T, the tau value was 28 μs. As the field strength increased to 14.1, 19.6, and 23.2 T, the tau value decreased to 20, 18 and 14 μs, respectively. On the other hand, the S/N ratio increased approximately proportional to B_o^2, as expected. The spectrum obtained at 23.2 T with 8 scans possess a S/N ratio a factor of 1.4 greater than the one obtained at 14.1 T with same number of scans.

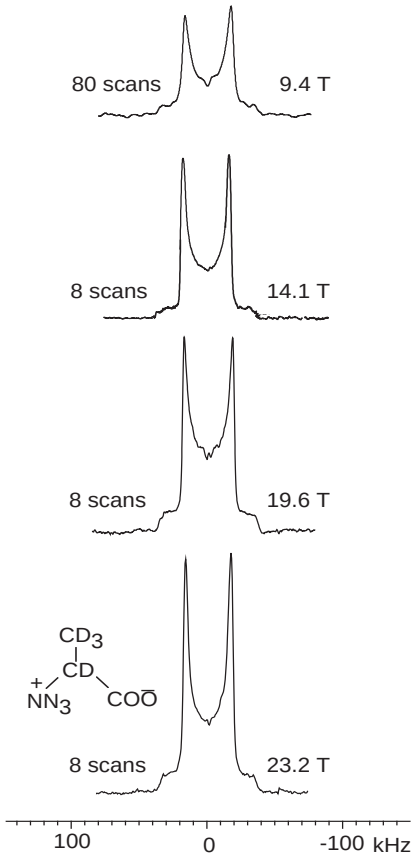

Figure 1. Deuterium spectra of 10 mg *d*4-alanine at 9.4, 14.1, 19.6 and 23.2 T. As the field increases, the S/N ratio increases for the same number of spins. This increase in sensitivity is one of the advantages of high fields for NMR.

High magnetic fields offer many advantages to NMR spectroscopy. Here, we have demonstrated the optimal increase of sensitivity with B_o strength, and in the case of deuterium spectroscopy, the minimization of tau that enables the detection of sites possessing short T_{2e} relaxation values.

References:

1 Soghomonian, V., *et al*., J. Mag. Res., 125, 212 (1997).

An Optically Pumped NMR Study of the Mechanism of Formation of Type-I Xenon Hydrate Clathrate

Storhaug, V., UF, Chemistry
Liebig, F., UF, Chemistry
Hughes, E., UF, Chemistry
Bowers, C.R., UF, Chemistry

The hydrate clathrates are a class of solids in which guest molecules occupy cages in a host structure formed from H-bonded water molecules. The normally unstable empty clathrate is stabilized by inclusion of the guest. While the general crystal structure of the type-I hydrate clathrates has already been established, the proposed mechanism for their nucleation and growth awaits experimental confirmation. This being our objective, we have studied both the melting and kinetics of formation of type I xenon hydrate clathrate using hyperpolarized ^{129}Xe NMR. The >2000-fold signal enhancement afforded by this method permits single scan observation of cage formation at less than parts-per-thousand levels. The signals arising from ^{129}Xe enclathrated in the tetrakaidecahedral (large) and dodecahedral (small) cages are well resolved, permitting the time dependence of each type to be measured independently.

Our kinetic model incorporates the time variations of the densities of the gaseous xenon, the xenon enclathrated into the small and large cages, and the ^{129}Xe magnetization of all three species. The

pressure and NMR data at 223 K support a mechanism whereby the hydrate nucleates by first forming a small cage. This nucleation site then serves as a template for the formation of large and additional small cages. It turns out that this mechanism is consistent with recent molecular dynamics simulations of the formation process.

The figure presents the ^{129}Xe NMR spectrum of xenon hydrate clathrate formed at T = 263 K. The theoretical cylindrically symmetric chemical shift powder pattern is superimposed on the experimental spectrum. The inset shows the time dependence of the signal integrals obtained for the large and small cages at T = 223 K. The kinetic model is represented by the solid lines through the data.

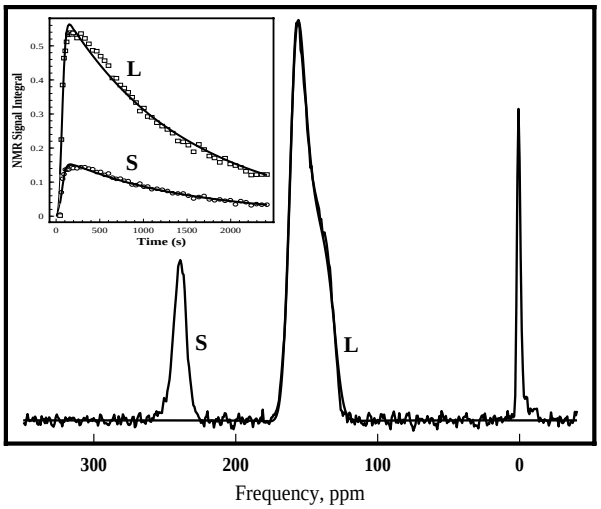

Figure 1. The hyperpolarized xenon-129 NMR spectrum of xenon hydrate clathrate formed at T = 263 K, along with simulation (solid line) of the large cage (L) chemical shift powder pattern. The inset presents the T = 233 K time dependence of the signal integral from the small (S) and large cages, with the solid line representing the kinetic model.

Magnetic-Field Perturbed NQR for Ultra-Low Temperature Thermometry

Sullivan, N.S., UF, Physics/NHMFL
Genio, E.B., Univ. of California, Santa Barbara, Physics
Ihas, G.G., UF, Physics/NHMFL

We have carried out measurements of the magnetic field perturbed nuclear quadrupole resonance (NQR) lines of powdered Sb immersed in liquid helium three at low temperatures. The magnetic field was used to separate the frequencies of the allowed transitions between the $I_Z = \pm 1/2$ and $\pm 3/2$ levels that correspond to the zero field NQR absorption at 11.5289 MHz. The spectrum for the powder sample consists of two sharp lines with known separation. The ratios of the intensities of these two lines depends only on the difference in thermal population of the nuclear spin levels and can be used for thermometry at very low temperatures. Pulsed NQR measurements of this intensity ratio from 0.25 to 1.45 mK were in good agreement with the expected Boltzmann distributions. Temperature resolutions of 20% could be achieved for signal integration times of the order of one hour.

This method of *Population Difference Thermometry* is very general and is based on the fact that inside the multiplet, the relative intensities depend only on the difference in thermal population of the nuclear spin levels between which the transitions occur. For use as a primary thermometer, we must consider only cases for which the transition matrix elements are all identical or precisely known from first principles. This would exclude systems where collective interactions appreciably perturb the intensities or the line shapes. With these conditions satisfied, the intensities of the transitions studied depend only on the temperature and the frequencies. Simple observations of the spectra can therefore, in principle, provide a measure of the temperature without need for calibration. For practical applications, the method has good

sensitivity when the energy separations of the levels becomes comparable to the temperature. For this reason, magnetic resonance transitions in the range of tens of MHz are particularly promising for thermometry in the sub-millikelvin range.

The dotted line in Figure 1 shows the theoretical intensity ratio for the two cusp singularities in the field-perturbed spectra of ^{121}Sb. The measured intensity ratio suggests a higher than expected intensity for the low frequency absorption line (or lower intensity for the high frequency line). This anomaly is attributed to the frequency dependence of the anomalous skin depth which varies as $\nu^{-1/3}$. At lower frequencies, the RF field penetrates further into the metal and samples more spins, and thus the intensity is higher than that of the high frequency line. The most reliable way to treat the data is to normalize the intensity ratio to the high temperature limit where the ratio must be unity. This normalized theoretical ratio is shown by the solid line in the figure which provides a good fit to the data. At the lowest temperature, 0.25 mK, the temperature uncertainty is about 0.05 mK. This precision could be improved by enhancing the signal/noise ratio for a given signal integration time.

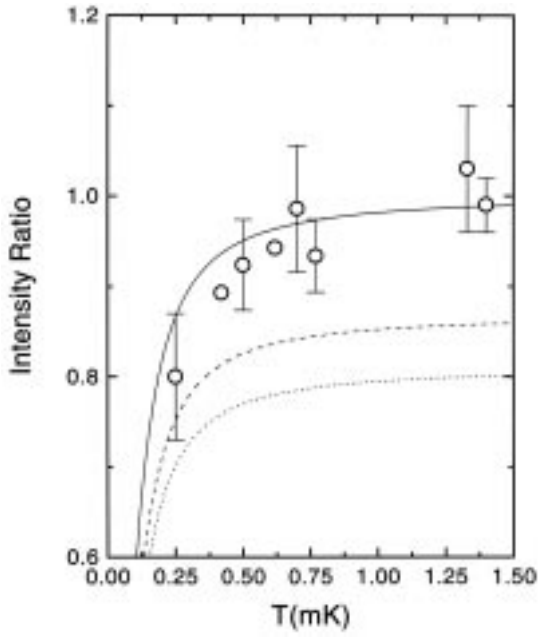

Figure 1. Observed temperature dependence of the intensities of the two peaks of the NMR spectrum for the magnetic field perturbed NQR resonances of ^{121}Sb.

Simple High-Magnetic-Field Probe for Superconducting Magnets

Xia, J.S., NHMFL/UF, Physics
Sullivan, N.S., NHMFL/UF, Physics
Adams, E.D., NHMFL/UF, Physics

Nuclear magnetic resonance techniques are clearly ideal for testing high field superconducting magnets, and in particular for probing the spatial homogeneity and temporal stability of the magnets. Nevertheless, this is not always standard practice because of the view that it is complicated and needs expensive equipment. Simple designs that are reliable and easy to use are available.

We used a small NMR probe consisting of powdered zeolite 1 with a slit cylinder of copper as a one turn coil to form a UHF NMR probe for characterizing a 16 T superconducting magnet. Helium three gas was adsorbed onto the zeolite to form a high-sensitivity (high magnetic moment), fast-relaxing sample with the probe held at 4 K. The miniature "coil" was resonated with a pair of non-magnetic capacitors (sealed against liquid helium) and connected as a capacitive transformer to simultaneously resonate at the desired frequency

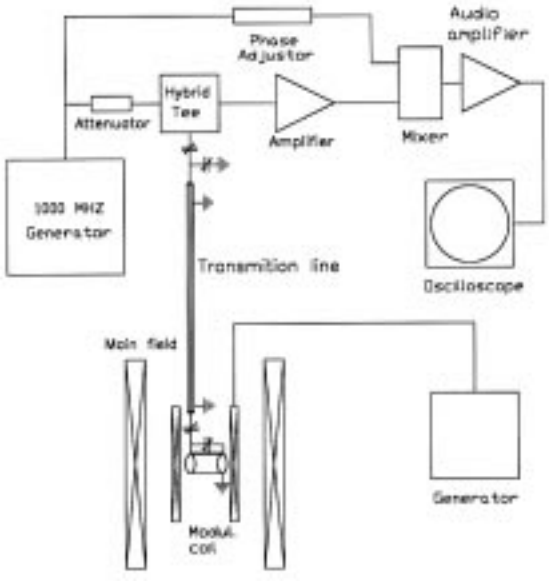

Figure 1. 500 MHz CW NMR spectrometer.

and to match a cryogenic 50-ohm coaxial cable. The cable was matched to an inexpensive quadruature hybrid tee that operated as a bridge with one port being the resonant circuit and the other a fixed 50-ohm termination. The difference between the arms of the bridge was amplified and detected to provide the observed resonances. The schematic of the spectrometer is shown in Figure 1.

The narrow resonance line of helium three was ideal for the calibrations. In principle the capacitors can be tuned to a desired frequency range and used for a relatively wide range of magnetic fields. If such a multipurpose probe were needed, it would be advantageous to use a more conventional coil and operate at lower frequency using sample with lower magnetic moments. Hydrogen, neon, and xenon also could be used as adsorbed samples in the probe.

Method for Removal of Magnetic Susceptibility Distortions in High-Field T_2*-Weighted Magnetic Resonance Imaging

Yang, Q.X., Penn State Univ., Radiology
Briggs, R.W., UF, Radiology/Chemistry/Biochemistry and Molecular Biology
Smith, M.B., Penn St. Univ., Radiology/Cellular and Molecular Physiology

Introduction. Development of high magnetic field MRI techniques for microimaging and *in vivo* imaging is hampered by the significant artifacts produced by B_0 inhomogeneities due to adjacent regions of differing magnetic susceptibility. Gradient Echo Slice Excitation Profile Imaging (GESEPI) has recently been introduced as a means of recovering signal lost to intravoxel phase dispersion originating from macroscopic susceptibility gradients in T_2*-weighted MR imaging, and demonstrated to work effectively at field strengths up to 9.4 T.[1] Our experiments at the NHMFL were designed to test the usefulness of the method for correcting susceptibility artifacts at the highest field currently available for MR imaging.

Methods. Mouse brain gradient-recalled echo (GRE) images in the coronal plane were acquired at 14 T on a Bruker 600 wide bore Avance at the NHMFL with TR = 100 ms, 1 mm slice thickness, 128 x 128 matrix, and 20 mm field of view (FOV). GESEPI images were acquired with 32 G_C steps per image set with $G_C^{max} = \pm$ 250%. Other images were acquired using similar parameters.

Results and Discussion. Figure 1 shows GRE and GESEPI images obtained of a phantom in a plane near an air-filled spherical capillary. Figure 2 shows 14 T images of a live mouse brain. In summary, GESEPI has been shown to effectively remove susceptibility-based intravoxel dephasing artifacts and signal loss in GRE images and to dramatically improve the quality of T_2*-weighted images even at long TE times and at high field strengths.[2] This method should be useful for obtaining T_2* contrast from

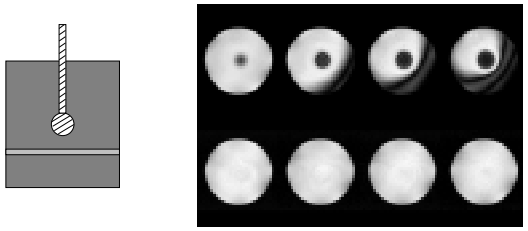

Figure 1. GRE (top) and GESEPI (bottom) phantom images in a plane near an air-filled sphere (insert, left). TE = 4, 10, 15, and 20 ms (left to right). B_0 = 14 T.

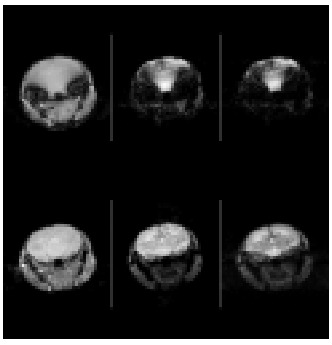

Figure 2. Live mouse brain GRE (top) and GESEPI (bottom) images. TE = 6, 15, and 20 ms (left to right).

microscopic intravoxel field variations without the deleterious influence of artifacts from local macroscopic field gradients resulting from susceptibility differences within the sample. It is also important for use in fast multi-slice imaging in high-field whole-body MRI, where conventional fast-spin echo (FSE) methods of obtaining rapid T_2-weighted images are severely compromised by rf power deposition (SAR) limitations, and substitution of T_2*-weighted multi-slice gradient echo sequences would otherwise be contaminated by severe susceptibility artifacts. Finally, it should benefit microimaging of small objects at very high magnetic field strengths.

References:

1 Yang, Q.X., *et al.*, Proc. ISMRM, 4, 1993 (1997).
2 Yang, Q.X., *et al.*, 38th ENC (Orlando, FL), abstract P-011 (1997).

Enhancement of the Effective Resolution of Mass Spectra of High-Mass Biomolecules by Maximum-Entropy Based Deconvolution to Eliminate the Isotopic Natural Abundance Distribution

Zhang, Z., NHMFL
Guan, S., NHMFL/FSU, Chemistry
Marshall, A.G., NHMFL/FSU, Chemistry

Although high-resolution Fourier transform ion cyclotron resonance mass spectrometry can resolve individual isotopic masses for biomolecules of more than 100 kDa, its effective mass accuracy is limited by the distribution of naturally occurring rare isotopes (^{13}C, ^{15}N, ^{18}O, ^{34}S, etc.). We recently compared least-squares and maximum-entropy methods for deconvolution of the isotopic natural abundance distribution to narrow the mass spectral isotopic abundance envelope for greatly enhanced effective mass resolution.[1] We have applied both methods to yield deconvolved high-resolution deuterium distributions for peptides and proteins subjected to H/D exchange prior to electrospray FT-ICR mass analysis (Figure 1). In addition, we showed that even unresolved isotopic envelopes from a quadrupole mass spectrometer can be narrowed for considerably improved resolution there as well.

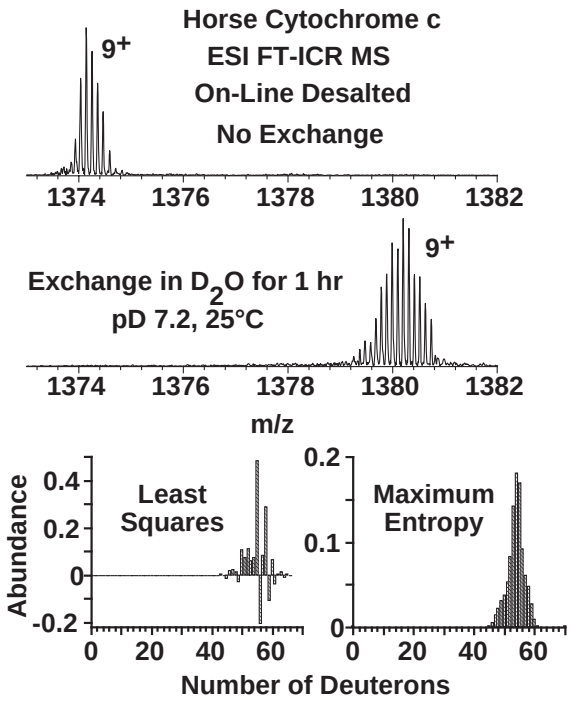

Figure 1. Electrospray FT-ICR 9.4 T mass spectra of horse heart cytochrome c before (top) and after (middle) exchange in D_2O solution (pH meter reading 7.2, 25 °C) for 1 hour. Bottom: Deuterium abundances calculated by least squares (left) and maximum-entropy (right) methods for the H/D-exchanged sample. Note the spurious negative abundances in least squares result.[1]

References:

1 Zhang, Z., *et al.*, J. Am. Soc. Mass Spectrom., 8, 659-670 (1997).